Analysis of Millimeter Wave Cellular Networks with Simultaneous Wireless Information and Power Transfer

Lam-Thanh Tu and Marco Di Renzo
Paris-Saclay University – Laboratory of Signals and Systems (UMR-8506)
CNRS – CentraleSupélec – University Paris-Sud
3 rue Joliot-Curie, 91192 Gif-sur-Yvette (Paris), France
e-mail: {lamthanh.tu, marco.direnzo}@l2s.centralesupelec.fr

***Abstract*— In this paper, we study the achievable performance of information decoding and harvested power in Simultaneous Wireless Information and Power Transfer (SWIPT) millimeter wave (mmWave) cellular networks. In particular, by modeling the Base Stations (BSs) as points of a Poisson Point Process (PPP) and by applying Maximum Ratio Transmission (MRT) and Maximum Ratio Combining (MRC) at the BSs and Mobile Terminals (MTs), respectively, the Joint Complementary Cumulative Distribution Function (JCCDF) of information rate and harvested power is analyzed. Our results show that mmWave cellular networks achieve better JCCDF performance than conventional microWave (μWave) cellular networks.**

I. Introduction

With the proliferation of smart devices and power-hungry high data rate applications, the need of efficiently using power and frequency resources is becoming increasingly important, leading to the well-known battery depletion and spectrum scarcity issues in the telecommunications industry.

To overcome the first challenge, energy harvesting has recently been proposed as a promising solution for prolonging the lifetime of the battery of low-energy devices without the need of increasing the size of the battery itself. A potential solution that is receiving prominence in the academic literature is the possibility of harvesting energy from ambient Radio Frequency (RF) signals, as opposed to other options that rely on harvesting energy from renewable energy resources, such as solar and wind powered BSs [1], [2].

RF-based energy harvesting paves the way for a new generation of communication networks, where the same transmitted waveform may be used, depending on the needs, either for transmitting data or as a vehicle for transferring energy. This communication paradigm is today known as Wireless Powered Communication (WPC). In WPC, the RF signals can be used not only for transmitting information but also for powering up the receiving devices. If the same RF signal is used for information transmission and for recharging the battery of low-energy devices, then it is referred to as Simultaneous Wireless Information and Power Transfer (SWIPT).

To overcome the second challenge, in addition, millimeter wave (mmWave) communication networks have received prominence due to the latest advances in high-frequency circuit design and are nowadays considered to be feasible for application to both indoor and outdoor scenarios [3]. To tackle the spectrum scarcity problem, as a result, a promising solution is to shift the carrier frequency of communication systems from the sub-6 GHz to the 30-300 GHz frequency range.

The great advantage of using mmWave frequencies is the abundance of available spectrum. The signals, however, are expected to undergo a larger path-loss than at microwave (μWave) frequencies, for a given transmission distance. This excess path-loss may be compensated, however, with the aid of large antenna arrays, since the higher the frequency is the more antennas can be packed in the same space. These antennas can be used for compensating the larger path-loss with a higher beamforming gain [4], [5].

In this context, the achievable performance of SWIPT-enabled wireless networks has been studied, to some extent, in the literature. In [6], a closed-form expression for the Probability Density Function (PDF) of end-to-end Signal-to-Noise Ratio (SNR) was derived and based on the derived PDF, the Bit Error Rate (BER) was analyzed. The rate-energy region of dual-hop Amplify-and-Forward (AF) relaying was studied in [7]. The impact of imperfect channel state information on the system performance was studied in [8]. These works, however, consider link-level performance, while the impact of large-scale interference is neglected.

Recently, few research works have investigated the potential of SWIPT-enabled cellular networks from the system-level standpoint [9]–[12]. In [9], the Joint Complementary Cumulative Distribution Function (JCCDF) of harvested power and rate was jointly considered by modeling the Mobile Terminals (MTs) and Base Stations (BSs) as points of two Poisson Point Processes (PPPs). In these papers, it was reported that there exists an optimum value of the density of BSs that maximizes the JCCDF. Even though the analysis in [9] is sufficiently general from the system-level standpoint, only single-antenna transmission at both the BSs and MTs is considered. In [11] and [12], on the other hand, mmWave cellular networks are not considered.

In this paper, we generalize the analysis in [9] along two main directions: we consider Multiple-Input-Multiple-Output

(MIMO) transmission and focus our attention on mmWave rather than microWave (μWave) cellular networks. Our analysis leverages the modeling approach proposed in [13], where, however, SWIPT is not taken into account, and generalizes it for Maximum Ratio Transmission (MRT) and Maximum Ratio Combining (MRC) at the BSs and MTs, respectively.

The rest of this paper is organized as follows. In Section II, the system model and problem formulation are introduced. In Section III, simulation results and design insight based on Monte Carlo simulations are provided. Finally, Section IV concludes this paper.

II. System Model

A. PPP–Based Cellular Networks Modeling

We consider a two-dimensional downlink cellular network, where the BSs are equipped with N_T antennas and are modeled according to a homogeneous PPP denoted by Ψ whose spatial intensity is λ_{BS}. The MTs are modeled as another homogeneous PPP with intensity λ_{MT}, which is independent of Ψ. The MTs are equipped with N_R antennas. We assume that $\lambda_{\text{MT}} \gg \lambda_{\text{BS}}$, so that the cellular network is fully-loaded, i.e., all the BSs are active and serve at least one MT in their coverage regions. Thanks to the Slivnyak theorem, the analysis is conducted for the typical MT located at the origin [14]. The typical MT is served by the BS providing the highest average received power to it. This serving BS is denoted by $\text{BS}^{(0)}$. The other BSs act as source of interference for the typical receiver. They are denoted by $\Psi^{(\backslash 0)} = \Psi \backslash \text{BS}^{(0)}$.

B. SWIPT-Enabled Cellular Networks

In our analysis, the typical MT [15, Fig. 3] has the inherent capability of not only being able to decode the intended signal, i.e., Information Decoding (ID), but it is also capable of harvesting the energy from the received signal with the aid of an Energy Harvesting (EH) module. In general, two operational schemes can be applied for this kind of receivers, i.e., time switching and power splitting. Time switching uses a portion of total transmission time for EH and the rest for ID. Power splitting splits the received signal in two parts, one is input to the EH receiver providing power $\text{P}_{\text{EH}} = \rho \text{P}_{\text{RX}}$, and the other is input to the ID receiver, $\text{P}_{\text{ID}} = (1-\rho)\,\text{P}_{\text{RX}}$, where ρ is the power splitting ratio, $0 \leq \rho \leq 1$, and P_{RX} is the received power. As proven in [9], the power splitting scheme outperforms the time switching scheme. In this paper, hence, we only consider the first scheme.

C. Channel Modeling

1) Multi-Ball LOS/NLOS Link State Modeling: The performance of SWIPT highly depends on the spatial blockages, e.g., the presence of buildings that may be in between the BSs and MTs in urban scenarios. In this case, the MTs may be either in Light-of-Sight (LOS) or in Non-LOS (NLOS) with respect to their serving and interfering BSs. In particular, a generic link is said to be in LOS if there is no blockage between the BS and MT, while it is said to be in NLOS if the link from the BS to the MT is blocked. Usually, the probability of a link to be in LOS or NLOS depends on the transmission distance between BS and MT: the larger the transmission distance is, the higher the probability that the link is in NLOS.

In this paper, we adopt the so-called multi-ball LOS/NLOS link state model which is accurate enough to realistically modeling LOS and NLOS links and, at the same time, is mathematically tractable. For further details about this model and its accuracy for representing actual blockages in urban scenarios, the interested readers may refer to [16] and [17].

Based on the multi-ball LOS/NLOS link state model, the distance between a generic BS and MT is split into $N+1$ regions, which correspond to N balls whose center is, e.g., the MT. Let $0 = d_0 < d_1 < d_2 < \cdots < d_N < d_{N+1} = \infty$ be the radii of the N balls. The probability of LOS/NLOS link can be formulated as follows:

$$p_s(r) = \sum_{n=1}^{N+1} q_s^{[d_{n-1},d_n]} \mathbf{1}_{[d_{n-1},d_n)}(r) \tag{1}$$

where $q_s^{[a,b]}$ for $s \in \{\text{LOS, NLOS}\}$ denotes the probability that a link of length $r \in [a,b]$ is in state s; $\mathbf{1}_{[d_{n-1},d_n)}$ is the generalized indicator function defined as $\mathbf{1}_{[d_{n-1},d_n)}(r) = 1$ if $r \in [a,b)$ and $\mathbf{1}_{[d_{n-1},d_n)}(r) = 0$ if $r \notin [a,b)$.

In this paper, a link can only be either in LOS or NLOS, so that the equality $\sum_{s\in\{\text{LOS,NLOS}\}} q_s^{[d_{n-1},d_n]} = 1$ for $n \in \{1, N+1\}$ holds.

By assuming that the LOS/NLOS status of each link is independent of the other links, the homogeneous PPP, Ψ, of the BSs can be divided into two independent and non-homogeneous PPPs, i.e., Ψ_{LOS}, Ψ_{NLOS}, such that $\Psi = \Psi_{\text{LOS}} \cup \Psi_{\text{NLOS}}$. This originates from the thinning theorem of the PPP. In particular, the densities of the two PPPs, Ψ_{LOS} and Ψ_{NLOS}, are $\lambda_{\text{LOS}}(r) = \lambda_{\text{BS}} p_{\text{LOS}}(r)$ and $\lambda_{\text{NLOS}}(r) = \lambda_{\text{BS}} p_{\text{NLOS}}(r)$.

2) Path-Loss Modeling: The path-loss of LOS and NLOS links is assumed to be the following:

$$l_{\text{LOS}}(r) = k_{\text{LOS}} r^{\beta_{\text{LOS}}} \quad l_{\text{NLOS}}(r) = k_{\text{NLOS}} r^{\beta_{\text{NLOS}}} \tag{2}$$

where k_{LOS} and k_{NLOS} are the path-loss constants of LOS and NLOS links; r denotes a generic BS-to-MT distance; β_{LOS} and β_{NLOS} denote the path-loss slopes of LOS and NLOS links, respectively.

3) Shadowing Modeling: In addition to the path-loss, we consider shadowing. It is assumed to follow a log-normal distribution with mean and standard deviation (in dB) equal to μ_s and to σ_s. In the rest of this paper, the notation $\mathcal{S}a(\mu_s, \sigma_s)$ is used for identifying the distribution.

4) Fading Modeling: Besides the impact of the distance-dependent path-loss and the shadowing, the transmission between a BS and a MT is impaired by small-scale fading. We assume a Nakagami-m distribution for the channel envelope, whose shape and spread parameters are denoted by m and Ω, respectively. In the rest of this paper, the notation $\mathcal{N}a(m,\Omega)$ is used for identifying the distribution. For simplicity, we consider independent and identically distributed (i.i.d.) fading, i.e., all the channels have the same shape and normalized spread parameter: $m_i = m, \Omega_i = 1, \forall_i \in \Psi$.

D. Directional Beamforming

In mmWave systems, highly directive antennas are expected to be used at both the BSs and MTs in order to overcome the larger path-loss due to using a high carrier frequency. Directional antennas, in addition, have the desirable bonus of reducing the other-cell interference. In practice, highly-directive radiation patterns are realized by using many antennas at the BSs and MTs. In this paper, for ease of mathematical tractability, we consider a two-lobe model for the radiation pattern, where φ_q is the beamwidth of the main lobe, and $G_{\max}$ and $G_{\min}$ are the beamforming gains of the main and side lobe, respectively. A more general modeling approach is available in [17].

Then, the antenna radiation pattern of BSs and MTs, g_{BS} and g_{MT}, can be formulated as follows:

$$g_q(\theta) = \begin{cases} G_{\max} & \text{if} \quad |\theta| \leq \varphi_q \\ G_{\min} & \text{if} \quad \varphi_q < |\theta| \leq \pi \end{cases} \tag{3}$$

where $q \in \{\text{BS},\text{MT}\}$, $\theta \in [-\pi, \pi)$ is the angle of the boresight direction.

The typical MT and its serving BS estimate the angles of arrival and departure, as well as adjust their antenna steering orientations accordingly. Thus, the antenna gain of the typical intended link is $G^{(0)} = G^{\text{BS}}_{\max} G^{\text{MT}}_{\max}$. As for the interfering links between the generic BS, $\text{BS}^{(i)}$, and the typical MT, the antenna gains are assumed to be randomly oriented, i.i.d., and uniformly distributed in $[0; 2\pi)$. They are denoted by $G^{(i)} = g_{\text{BS}}(\theta_i)\, g_{\text{MT}}(\theta_{i,\text{MT}})$ where θ_i are $\theta_{i,\text{MT}}$ the angles of the boresight direction at the BS and MT.

E. Cell Association Criterion

The typical MT is served by the BS that provides the highest long-term received power. Thus, path-loss and shadowing are taken into account for cell association. We denote by $\mathcal{W}^{(0)}$ the highest long-term received power, which is defined as follows:

$$\mathcal{W}^{(0)} = \max\left\{\mathcal{W}^{(0)}_{\text{LOS}}, \mathcal{W}^{(0)}_{\text{NLOS}}\right\}, \mathcal{W}^{(0)}_s = \max_{i\in\Psi_s}\left\{\mathcal{W}^{(i)} = \frac{\text{Sa}^{(i)}_s}{k_s r_i^{\beta_s}}\right\} \tag{4}$$

where $\max\{\cdot\}$ is the maximum function.

F. MRT/MRC Transmission

The BSs and the MTs are assumed to use MRT and MRC, respectively. From [18], the received signal at the typical MT can be formulated as follows:

$$\begin{aligned}\mathbf{y} =& \sqrt{PG^{(0)}\frac{\text{Sa}^{(0)}}{k_0 r_0^{\beta_0}}}\mathbf{H}_0\mathbf{w}_{T,0}s_0 \\ &+ \sum_{i\in\Psi^{(\setminus 0)}}\sqrt{PG^{(i)}\frac{\text{Sa}^{(i)}}{k_i r_i^{\beta_i}}}\mathbf{H}_i\mathbf{w}_{T,i}s_i + \mathbf{m}\end{aligned} \tag{5}$$

where $\mathbf{y} \in \mathbb{C}^{N_R\times 1}$; $\beta_0, \beta_i \in \{\beta_{\text{LOS}}, \beta_{\text{NLOS}}\}$; s_0 and s_i are the transmitted symbols of serving and interfering BSs with $\mathbb{E}\left\{|s_0|^2\right\} = \mathbb{E}\left\{|s_i|^2\right\} = 1$; $\mathbb{E}\{\cdot\}$ is expectation operator; $\mathbf{H}_0$ and $\mathbf{H}_i \in \mathbb{C}^{N_R\times N_T}$ are the channel matrices of the intended and interfering links respectively, whose entries are $\mathbf{H}_0^{(r,t)}$ and $\mathbf{H}_i^{(r,t)} \sim \mathcal{N}a(m,1)$, (Sec. II-C.4) for $r = 1,\ldots,N_R$, $t = 1,\ldots,N_T$; P is the transmit power of all BSs; $\text{Sa}^{(0)}$ and $\text{Sa}^{(i)}$ are the shadowing gains of intended and interfering BSs (Sec. II-C.3); $\mathbf{w}_{T,0}$ and $\mathbf{w}_{T,i}$ are the transmit beamsteering vectors of the serving and interfering BSs, which are the eigenvectors corresponding to the largest eigenvalue χ_0 of $\mathbf{F}_0 = \mathbf{H}_0^*\mathbf{H}_0$ and χ_i of $\mathbf{F}_i = \mathbf{G}_i^*\mathbf{G}_i$; $\mathbf{G}_i$ is the channel matrix of the link between $\text{BS}^{(i)}$, for $i \in \Psi^{(\setminus 0)}$, and its serving MT; $\mathbf{m} \in \mathbb{C}^{N_R\times 1}$, $\mathbf{m}^{(r)} \sim \mathcal{CN}\left(0, \sigma^2_{\text{NC}}\right)$, is the additive white Gaussian noise at the receiver, where $\mathcal{CN}\left(0,\sigma^2\right)$ denotes a complex Gaussian random variable with zero mean and variance σ^2.

At the MTs, the signals are multiplied by the normalized decoding vector $\mathbf{w}_{R,0} = \frac{\mathbf{H}_0\mathbf{w}_{T,0}}{\|\mathbf{H}_0\mathbf{w}_{T,0}\|}$, according to the MRC scheme. Thus, the intended signal, $\mathcal{U}^{(0)}$, and the other-cell interference at the EH receiver, $\text{I}^{\text{EH}}_{\text{agg}}$, and at the ID receiver, $\text{I}^{\text{ID}}_{\text{agg}}$, receiver can be written as follows:

$$\begin{aligned}\mathcal{U}^{(0)} =& \frac{G^{(0)}\chi_0\text{Sa}^{(0)}}{k_0 r_0^{\beta_0}} \\ \text{I}_{\text{agg}} =& \text{I}^{\text{EH}}_{\text{agg}} = \text{I}^{\text{ID}}_{\text{agg}} = \sum_{i\in\Psi^{(\setminus 0)}}\frac{\text{Sa}^{(i)}G^{(i)}}{k_i r_i^{\beta_i}\chi_0}\left\|(\mathbf{H}_0\mathbf{w}_{T,0})^*\mathbf{H}_i\mathbf{w}_{T,i}\right\|^2 \\ \chi_0 =& (\mathbf{H}_0\mathbf{w}_{T,0})^*\mathbf{H}_0\mathbf{w}_{T,0}.\end{aligned} \tag{6}$$

G. Problem Formulation

In this paper, we are interested in studying the potential of the MT of jointly harvesting power and transmitting data at a given rate. The harvested power is denoted by $\mathcal{Q}$ and the rate is denoted by $\mathcal{R}$. In particular, we study the JCCDF of harvested power and rate:

$$\begin{aligned}\mathcal{F}_c(\mathcal{Q}_*, \mathcal{R}_*) =& \Pr\{\mathcal{Q} \geq \mathcal{Q}_*, \mathcal{R} \geq \mathcal{R}_*\} \\ \mathcal{Q} =& \rho\xi\left(P\mathcal{U}^{(0)} + P\text{I}^{\text{EH}}_{\text{agg}}\right) \\ \mathcal{R} =& \text{BW}\log_2(1 + \text{SINR}) \\ \text{SINR} =& \frac{P\mathcal{U}^{(0)}}{P\text{I}^{\text{ID}}_{\text{agg}} + \sigma^2_{\text{NC}}}\end{aligned} \tag{7}$$

where ξ, $0 \leq \xi \leq 1$, denotes the conversion efficiency of the EH receiver; $\mathcal{Q}_*$ and $\mathcal{R}_*$ are the minimum power and rate requirements for the typical MT to be able to perform its tasks; BW is the transmission bandwidth; $\sigma^2_{\text{NC}} = \sigma^2_{\text{N}} + \sigma^2_{\text{C}}$, where σ^2_{N} is the thermal noise power defined as $\sigma^2_{\text{N}} = 10^{\sigma^2_{\text{N}}(\text{dBm})/10}$ with $\sigma^2_{\text{N}}(\text{dBm}) = -174 + 10\log_{10}(\text{BW}) + \mathcal{F}_{\text{dB}}$ and $\mathcal{F}_{\text{dB}}$ being the noise figure in dB, and $\sigma^2_{\text{C}} = \frac{\sigma^2_{\text{cov}}}{1-\rho}$ with σ^2_{cov} taking into account the noise introduced during the conversion from radio frequency to baseband.

III. Simulation Results

In this section, two mmWave cellular networks with carrier frequency equal to 28 GHz and 73 GHz, $f_c = \{28, 73\}$ GHz, are considered. Without otherwise stated, the same simulation parameters as in [19] are used. More precisely:

- The path-loss model is as follows: $\beta_{\text{LOS}} = 2$, $\beta_{\text{NLOS}} = 2.92$, $k_{\text{LOS}} = 61.4$ dB and $k_{\text{NLOS}} = 72$ dB if $f_c = 28$ GHz and $\beta_{\text{LOS}} = 2$, $\beta_{\text{NLOS}} = 2.69$, $k_{\text{LOS}} = 69.8$ dB and $k_{\text{NLOS}} = 82.7$ dB if $f_c = 73$ GHz.
- The shadowing model is as follows: $\mu_{\text{LOS}} = \mu_{\text{NLOS}} = 0$ dB, $\sigma_{\text{LOS}} = 5.8$ dB and $\sigma_{\text{NLOS}} = 8.7$ dB if $f_c = 28$ GHz and $\sigma_{\text{LOS}} = 5.8$ dB and $\sigma_{\text{NLOS}} = 7.7$ dB if $f_c = 73$ GHz.
- The blockage model is as follows: $d_1 = 16.4312$ m, $d_2 = 74.8118$ m and $d_3 = 243.1534$ m, $q_{\text{LOS}}^{[0,d_1]} = 0.823$, $q_{\text{LOS}}^{[d_1,d_2]} = 0.3131$, $q_{\text{LOS}}^{[d_2,d_3]} = 0.06$ and $q_{\text{LOS}}^{[d_3,\infty]} = 0$ if $f_c = 28$ GHz; $d_1 = 16.1934$ m, $d_2 = 73.0481$ m and $d_3 = 236.0502$ m, $q_{\text{LOS}}^{[0,d_1]} = 0.8275$, $q_{\text{LOS}}^{[d_1,d_2]} = 0.3177$, $q_{\text{LOS}}^{[d_2,d_3]} = 0.0637$ and $q_{\text{LOS}}^{[d_3,\infty]} = 0$ if $f_c = 73$ GHz. The probability of NLOS is computed as $q_{\text{NLOS}}^{[a,b]} = 1 - q_{\text{LOS}}^{[a,b]}$.
- The transmission bandwidth is BW = 2 GHz. The noise power is $\sigma_N^2 = -174 + 10\log_{10}(\text{BW}) + \mathcal{F}_{\text{dB}}$, where $\mathcal{F}_{\text{dB}} = 10$ dB is the noise figure and σ_{cov}^2 = - 70 dBm; the energy conversion efficiency is $\xi = 0.8$ and the transmit power is $P = 30$ dBm.
- The directional beamforming model is as follows: $G_{\max}^{\text{BS}} = G_{\max}^{\text{MT}} = 20$ dB, $G_{\min}^{\text{BS}} = G_{\min}^{\text{MT}} = -10$ dB and $\varphi_{\text{BS}} = \varphi_{\text{MT}} = 30$ degrees.
- The scale and spread parameter of Nakagami-m fading are as follows: $m_{\text{LOS}} = 10$, $m_{\text{NLOS}} = 1$ and $\Omega_{\text{LOS}} = \Omega_{\text{NLOS}} = 1$.
- The density of BSs is $\lambda_{\text{BS}} = \frac{1}{\pi \text{Rcell}^2}$, where Rcell is the radius of a generic cell (in meter).

As far as μWave cellular networks are concerned, the following setup is considered: $f_c = 2.5$ GHz, BW $= 40$ MHz, $G_{\max}^{\text{MT}} = G_{\min}^{\text{MT}} = 0$ dB, the path-loss model is $l(r) = 22.7 + 36.7\log_{10}(r) + 26\log_{10}(2.5)$ in dB. All links are assumed to be in NLOS, and the standard derivation of shadowing is $\sigma_{\text{NLOS}} = 4$ dB. The other parameters are the same as for the mmWave setup.

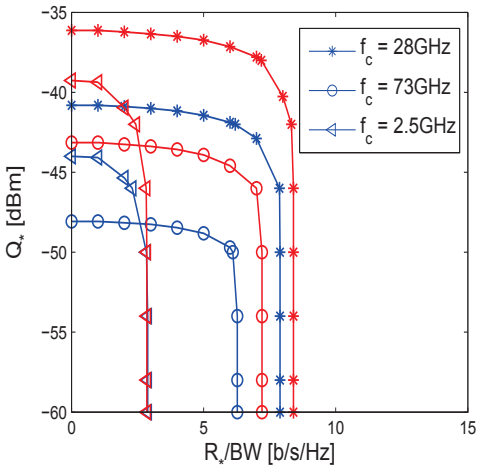

Fig. 1. Feasiblity regions for J-CCDF = 0.85. Blue curves: $N_T = 16$; Red curves: $N_T = 48$; N_R = 4; $\rho = 0.5$.

Figures 1 and 2 illustrate the feasibility regions if the JCCDF is equal to 0.85, $\mathcal{F}_c = 0.85$, i.e., the pairs of harvested power and rate that satisfy the requirement imposed on the JCCDF. We note that increasing the number of transmit and receive antennas enlarges the feasibility region. These figures also show that mmWave cellular networks can outperform μWave cellular networks, especially if $f_c = 28$ GHz.

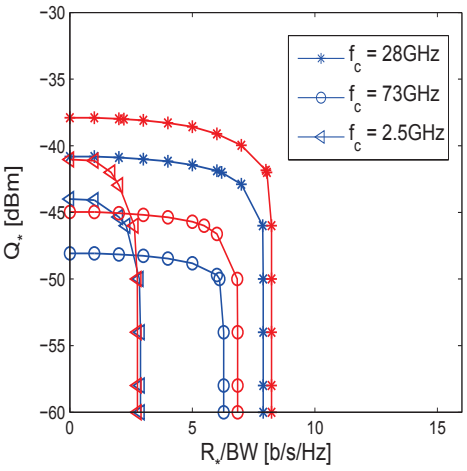

Fig. 2. Feasiblity regions for J-CCDF = 0.85. Blue curves: $N_R = 4$; Red curves: $N_R = 8$; N_T = 16; $\rho = 0.5$.

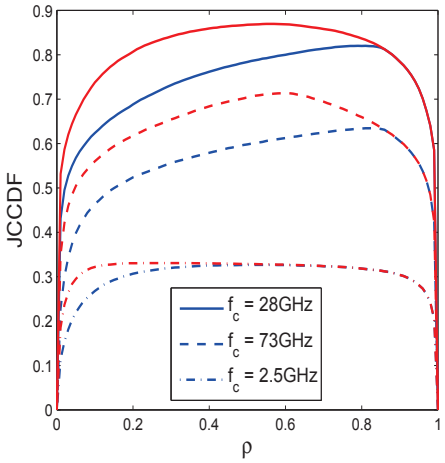

Fig. 3. J-CCDF vs. ρ; $N_T = 16$, $N_R = 4$. Blue curves are for $\left(Q_*, \frac{R_*}{\text{BW}}\right) = (-40, 7.5)$ and red curves are for $\left(Q_*, \frac{R_*}{\text{BW}}\right) = (-45, 7.5)$; Q_* in dBm; $\frac{R_*}{\text{BW}}$ in b/s/Hz.

Figure 3 illustrates the impact of the power splitting ratio, ρ, on the achievable JCCDF. From Fig. 3, we note that an optimal value of ρ that maximizes the JCCDF exists. This performance trends originates from the fact that the harvested power increases with ρ while the rate decreases with ρ. Once again, the mmWave cellular network at $f_c = 28$ GHz outperforms the other case studies.

Figure 4 depicts the impact of the density of BSs on the JCCDF. Due to the different blockage model that is considered for mmWave and μWave cellular networks, we observe a net

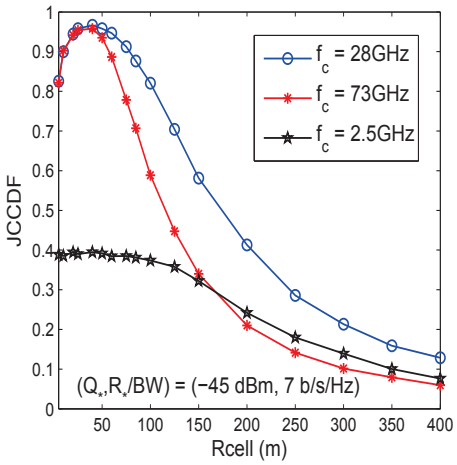

Fig. 4. J-CCDF vs. Rcell with $N_T = 16$; $N_R = 4$; $\rho = 0.5$.

difference of the impact of network densification. As far as mmWave cellular networks are concerned, an optimal value of the density of BSs, or Rcell, exists, which depends on the blockage model itself. As far as μWave cellular networks are concerned, on the other hand, we note that increasing the density of BSs has no negative impact on the JCCDF. Beyond a certain density, however, no gain is obtained by further increasing the number of BSs.

IV. Conclusion

In this paper, the JCCDF of information rate and harvested power of SWIPT-enabled mmWave cellular networks has been analyzed. The numerical results illustrate that the use of mmWave frequencies has the potential of increasing the amount of harvested power and achievable rate compared with μWave cellular networks.

Acknowledgment

This work is supported in part by the European Commission through the H2020-ETN-5Gwireless project under grant 641985.

References

[1] R. Zhang, R. G. Maunder, and L. Hanzo, "Wireless information and power transfer: From scientific hypothesis to engineering practice," *IEEE Commun. Mag.*, vol. 53, no. 8, pp. 99–105, Aug. 2015.

[2] O. Ozel, K. Tutuncuoglu, S. Ulukus, and A. Yener, "Fundamental limits of energy harvesting communications," *IEEE Commun. Mag.*, vol. 53, no. 4, pp. 126–132, Apr. 2015.

[3] T. S. Rappaport *et al.*, "Millimeter wave mobile communications for 5g cellular: It will work!" *IEEE Access*, vol. 1, pp. 335–349, May 2013.

[4] L. Zheng and D. N. C. Tse, "Diversity and multiplexing: a fundamental tradeoff in multiple-antenna channels," *IEEE Trans. Inf. Theory*, vol. 49, no. 5, pp. 1073–1096, May 2003.

[5] A. Goldsmith, S. A. Jafar, N. Jindal, and S. Vishwanath, "Capacity limits of MIMO channels," *IEEE J. Sel. Areas Commun.*, vol. 21, no. 5, pp. 684–702, Jun. 2003.

[6] L. Mohjazi, S. Muhaidat, and M. Dianati, "Performance analysis of differential modulation in SWIPT cooperative networks," *IEEE Signal Process. Lett.*, vol. 23, no. 5, pp. 620–624, May 2016.

[7] F. Benkhelifa and M. S. Alouini, "Simultaneous wireless information and power transfer for MIMO amplify-and-forward relay systems," in *GLOBECOM'15*, San Diego, CA, Dec. 2015, pp. 1–6.

[8] C. F. Liu, M. Maso, S. Lakshminarayana, C. H. Lee, and T. Q. S. Quek, "Simultaneous wireless information and power transfer under different csi acquisition schemes," *IEEE Trans. Wireless Commun.*, vol. 14, no. 4, pp. 1911–1926, Apr. 2015.

[9] M. Di Renzo and W. Lu, "System-level analysis/optimization of cellular networks with simultaneous wireless information and power transfer: Stochastic geometry modeling," *IEEE Trans. Veh. Technol.*, IEEE Early Access.

[10] W. Lu and M. Di Renzo and T. Q. Duong, "On stochastic geometry analysis and optimization of wireless-powered cellular networks," in *GLOBECOM'15*, San Diego, CA, Dec. 2015, pp. 1–7.

[11] L. T. Tu and M. Di Renzo and J. P. Coon, "System-level analysis of swipt mimo cellular networks," *IEEE Commun. Lett.*, vol. 20, no. 10, pp. 2011 – 2014, Oct. 2016.

[12] ——, "System-level analysis of receiver diversity in swipt-enabled cellular networks," *J. Commun. Netw.*, 2016, accepted.

[13] M. Di Renzo, "Stochastic geometry modeling and analysis of multi-tier millimeter wave cellular networks," *IEEE Trans. Wireless Commun.*, vol. 14, no. 9, pp. 5038–5057, Sep. 2015.

[14] M. Di Renzo and A. Guidotti and G. E. Corazza, "Average rate of downlink heterogeneous cellular networks over generalized fading channels: A stochastic geometry approach," *IEEE Trans. Commun.*, vol. 61, no. 7, pp. 3050–3071, Jul. 2013.

[15] A. A. Nasir, X. Zhou, S. Durrani, and R. A. Kennedy, "Relaying protocols for wireless energy harvesting and information processing," *IEEE Trans. Wireless Commun.*, vol. 12, no. 7, pp. 3622–3636, Jul. 2013.

[16] W. Lu and M. Di Renzo, "Stochastic geometry modeling of cellular networks: Analysis, simulation and experimental validation," *ACM MSWiM*, pp. 179–188, Nov. 2015.

[17] M. Di Renzo and W. Lu and P. Guan, "The intensity matching approach: A tractable stochastic geometry approximation to system-level analysis of cellular networks," *IEEE Trans. Wireless Commun.*, vol. 15, no. 9, pp. 5963 – 5983, Sep. 2016.

[18] M. Kang and M. S. Alouini, "A comparative study on the performance of MIMO MRC systems with and without cochannel interference," *IEEE Trans. Commun.*, vol. 52, no. 8, pp. 1417–1425, Aug. 2004.

[19] W. Lu and M. Di Renzo, "Stochastic geometry modeling of mmwave cellular networks: Analysis and experimental validation," in *IEEE Int. Workshop Measurement & Networking (M&N)*, Coimbra, Portugal, Oct. 2015, pp. 1–4.